Available online at www.sciencedirect.com
ScienceDirect
Earth and Planetary Science Letters 268 (2008) 245–254
EPSL
www.elsevier.com/locate/epsl

Testing the relationship between timing of geomagnetic reversals/excursions and phase of orbital cycles using circular statistics and Monte Carlo simulations

Chuang Xuan *, James E.T. Channell

Department of Geological Sciences, University of Florida, 241 Williamson Hall, P.O. Box 112120, Gainesville, Florida 32611, USA

Received 9 October 2006; received in revised form 3 October 2007; accepted 20 December 2007
Available online 11 January 2008
Editor: C.P. Jaupart

Abstract

Fuller (Fuller, M., Geomagnetic field intensity, excursions, reversals and the 41,000-yr obliquity signal, Earth Planet. Sci. Lett. 245 (2006) 605–615.) pointed out that, for 9 reversals over the last 3 Myr, reversal age has a non-random relationship to the phase of orbital obliquity. Our analysis, based on Rayleigh tests, indicates that reversals have no preferred phase distribution in the obliquity cycle at the 5% significance level over the last 3 Myr. There is, however, a statistically significant relationship (at the 5% level) between reversal age and the phase of orbital eccentricity for the last 3 Myr, although this relationship breaks down on adding just a few reversals beyond 3 Ma. Over the last 5 Myr, reversals preferentially occurred during decrease of the maximum obliquity envelope although, yet again, the relationship does not hold as additional reversals are added to the analysis, no matter which timescale is tested. The Rayleigh tests are all based on the assumption of no uncertainty in reversal/excursion age, or in orbital solutions. Monte Carlo simulations indicate that reversal/excursion ages would have to be known within 5–10 kyr to resolve a preferred phase in obliquity similar to that advocated by Fuller (Fuller, M., Geomagnetic field intensity, excursions, reversals and the 41,000-yr obliquity signal, Earth Planet. Sci. Lett. 245 (2006) 605–615.) over the last 3 Myr. Reversal/excursion ages would have to be known within ~15 kyr to resolve a preferred phase in orbital eccentricity for reversals over the last 3 Myr, and within ~40 kyr for the last 25 Myr. Comparison of astrochronological reversal timescales indicates that reversal age uncertainties exceed these limits, making it unlikely that a relationship of reversal/excursion age to the phase of obliquity or eccentricity would be resolvable. In the case of the obliquity envelope, the critical levels of reversal age uncertainty (~50 kyr for 0–3 Ma, ~200 kyr for 0–5 Ma, and ~400 kyr for 0–25 Ma) are less stringent. The presence of a significant relationship between reversal age and phase of the obliquity envelope for the last 5 Myr, but not further back in time, implies either larger than expected reversal age uncertainties in pre-Pliocene polarity timescales *and* a link between reversal age and the obliquity envelope, or, more probably, the fortuitous occurrence of a low probability relationship over the last 5 Ma that has no mechanistic implication.

Keywords: Geodynamo; Orbital forcing; Obliquity; Eccentricity; Reversals; Excursions

1. Introduction

There has been intermittent interest in the influence of orbital periods on the geomagnetic field that can be traced back to Blackett's experiments in the 1950s (Blackett, 1952). Geodynamos driven by precessional forces were advocated in the 1960s (e.g. Malkus, 1968) and are still thought to be viable (e.g. Vanyo and Dunn, 2001; Tilgner, 2005), although Rochester et al. (1975) and Loper (1975) have argued that the energy available from precession is insufficient to drive the geodynamo. Orbital periods in sedimentary relative paleointensity records have been considered evidence for orbital influence on the geodynamo (Kent and Opdyke, 1977; Channell et al., 1998; Yamazaki, 1999; Yamazaki and Oda, 2002). Orbital periods in paleomagnetic data may, however, be attributed to lithologic/climatic contamination

* Corresponding author.
E-mail address: xuan2005@ufl.edu (C. Xuan).

0012-821X/$ - see front matter © 2008 Elsevier B.V. All rights reserved.
doi:10.1016/j.epsl.2007.12.021

of the sedimentary relative paleointensity records (Kent, 1982; Guyodo et al., 2000; Roberts et al., 2003).

Kent and Carlut (2001) found no discernable tendency for reversals or excursions to occur at a consistent amplitude or phase of obliquity or eccentricity by comparing the histogram of obliquity and eccentricity values corresponding to ages of the last 21 reversals and 6 excursions in the Brunhes Chron with the histogram of orbital parameters over the same age ranges. These authors used the Lourens et al. (1996) polarity timescale for the last 5.5 Myrs, the Brunhes excursion chronologies of Langereis et al. (1997), and astronomical solutions from Laskar (1990). Fuller (2006) has recently revived the debate by comparing the timing of polarity reversals with current orbital solutions for obliquity (Laskar et al., 2004), utilizing the ATNTS2004 timescale (Lourens et al., 2004). Fuller (2006) determined the phase of the obliquity signal at time of reversal, and, for the last nine reversals covering the last 3 Myr, demonstrated that reversals preferentially occurred during decrease from maxima within the 41 kyr obliquity cycle (Fig. 7 of Fuller, 2006). After comparing the occurrence of the last 17 reversals with the smoothed maximum obliquity envelope, he also suggested that reversals preferentially occur when the average amplitude of the obliquity signal is lower than the mean. In addition, he noted a coincidence of paleointensity minima in the Sint-800 relative paleointensity stack (Guyodo and Valet, 1999) with minima in the orbital solution for obliquity, and a preferred duration of 30–40 kyr (corresponding to an obliquity cycle) for polarity subchrons in the last 13 Myr of the ATNTS2004 timescale (Lourens et al., 2004).

Here, we expand on Fuller's analysis by assessing the relationship of reversal/excursion age to the phase of orbital obliquity, the phase of the obliquity envelope, and the phase of eccentricity. Through Monte Carlo simulations, we provide estimates of the sensitivity of these results to reversal/excursion age uncertainties.

2. Data

The orbital solutions used here are those for obliquity and eccentricity from Laskar et al. (2004). This recent La2003 integration (Laskar et al., 2004) has been improved with respect to La93 (Laskar et al., 1993) by using direct integration of the gravitational equations for orbital motions, and by improving the dissipative contributions. For eccentricity, the solution is considered to be precise over the last 40 Myr because eccentricity depends on the orbital part of the solution (Laskar et al., 2004; Pälike et al., 2004). The solution for precession and obliquity is, however, less accurate due to the uncertainties that remain from tidal dissipation in the Earth–Moon system, which manifests largely as a small change in precession frequency, and appears in the obliquity solution as a time offset. Lourens et al. (2004) provided an estimate for uncertainty in the astronomic solution due to tidal dissipation by plotting the differences in age of correlative minimum values in the obliquity and precession cycles between two La2003 solutions that include the present-day and half the present-day tidal dissipation value for the last 25 Myr. According to this analysis, errors in astronomical ages over the last 10 Myr should be of the order of 0.1–0.2% (10–20 kyr) and possibly even less. At ~23 Ma, the differences between the two solutions reach three cycles, which correspond to a maximum uncertainty of ~68 kyr in precession, or ~123 kyr in obliquity (Fig. 21.7 in Lourens et al., 2004). Laskar et al. (2004) expected the solution for obliquity to be valid over the last 20 Myr with a 5% error in tidal dissipation; however, the error may increase to 10% beyond 20 Ma. An uncertainty of 10% in the tidal dissipation term corresponds to an uncertainty in the orbital solution of ~16 kyr after 20 Ma, and ~63 kyr after 40 Ma (Laskar et al., 2004). This implies an uncertainty of <16 kyr due to tidal dissipation in the orbital solution for obliquity during the last 20 Myrs.

For the last 15 years, the Cande and Kent (CK95) polarity timescale (Cande and Kent, 1992, 1995) has been the standard for stratigraphic studies dealing with the last 80 Myr. The 1995 version of this timescale utilized astrochronologically determined reversal ages for the last 5 Myrs (Shackleton et al., 1990; Hilgen, 1991) and radiometrically-calibrated marine magnetic anomaly (MMA) spacings prior to 5 Ma. The ATNTS2004 timescale (Lourens et al., 2004) for the Cenozoic incorporates many of the astrochronological timescale calibrations that have become available since 1995. Since the publication of ATNTS2004, the timescale of Billups et al. (2004) provides alternative age constraints in the 15–25 Ma interval from tuning of the oxygen isotope record at ODP Site 1090 (South Atlantic). Astronomically calibrated reversal ages from equatorial Pacific at ODP Site 1218 (Pälike et al., 2006) also cover the 15–25 Ma interval. Recently assigned astronomical ages with very small estimated uncertainties for reversal boundaries between 8.5 Ma and 12.5 Ma are based on the Monte dei Corvi section in northern Italy (Husing et al., 2007). Additional estimates of reversal ages for part of this interval (9.3–11.2 Ma) are available for eight polarity chron boundaries recorded at ODP Site 1092 from the South Atlantic (Evans et al., 2007). We utilize these six polarity timescales spanning different time intervals, and a compilation of excursion ages (Table 1), to test the relationship between the ages of reversals and excursions and the phases of obliquity, of eccentricity, and of the envelope of obliquity.

The main uncertainties in astronomically tuned reversal ages depend on the accuracy of the astronomical solution from which the target was derived, the accuracy of the tuning, and any lag between orbital forcing and response. To gauge uncertainties in polarity timescales, we plot the age differences between the six polarity timescales cited above, including the Shackleton et al.

Table 1
Ages of the 8 best-established excursions in the Brunhes and Matuyama chrons

Excursion name	Estimated age (ka)	Principal references
Mono Lake	33	Benson et al. (2003)
Laschamp	41	Laj et al. (2000)
Blake	120	Tric et al. (1991)
Iceland Basin	188	Channell (1999), Channell et al. (1997)
Pringle Falls	211	Singer et al. (in press)
Kamakatsura	850	Channell et al. (2002), Singer et al. (2004)
Santa Rosa	932	Channell et al. (2002), Singer et al. (2004)
Punaruu	1115	Channell et al. (2002), Singer et al. (2004)

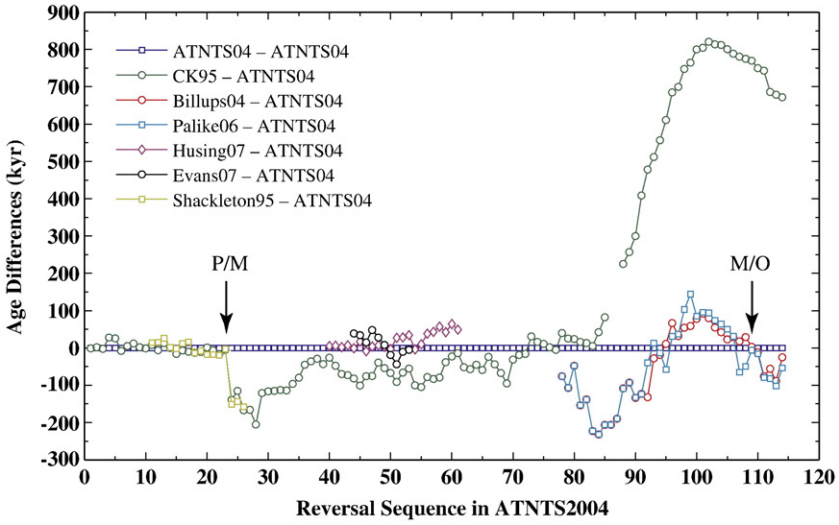

Fig. 1. Comparing differences in different reversal time scales (Lourens et al., 2004; Cande and Kent, 1995; Billups et al., 2004; Pälike et al., 2006; Husing et al., 2007; Evans et al., 2007; Shackleton et al., 1995) relative to ATNTS2004 time scale (Lourens et al., 2004). P/M denotes the Pliocene–Miocene boundary at ~5.332 Ma, and M/O denotes Miocene–Oligocene boundary at ~23.030 Ma.

(1995) timescale from ODP Leg 138 (equatorial Pacific), and the ATNTS2004 timescale (Fig. 1). For the last ~5 Myrs, differences among ATNTS2004, CK95, and the Shackleton et al. timescale are quite small (<50 kyr). Reversal ages in CK95 prior to 5 Ma were not astronomically determined, and differences between CK95 and ATNTS2004 exceed 800 kyr in the early Miocene. Differences among astronomically calibrated reversal timescales (Lourens et al., 2004; Billups et al., 2004; Pälike et al., 2006; Husing et al., 2007; Evans et al., 2007) reach 200 kyr in the Miocene (Fig. 1).

3. Methods

3.1. Phase calculation

To determine if the reversals and excursions occur at a preferred phase of orbital cycles (obliquity or eccentricity), we calculate the phase corresponding to reversals and excursions since 25 Ma with the definition of 'phase' as follows. The local maximum of obliquity or eccentricity is defined as 0°, the following local minimum is defined as 180°, and the following local maximum as 360°. If a reversal or excursion occurs at time T, which is between a local maximum at time T_1 and a local minimum at time T_2 (Fig. 2), the phase corresponding to that reversal or excursion can then be calculated using the following equation:

$$\alpha = \begin{cases} 180^{\circ} \times (T_1 - T)/(T_1 - T_2) & \text{If } T_1 \text{ is older than } T_2; \\ 180^{\circ} + \left(180^{\circ} \times (T_2 - T)/(T_2 - T_1)\right) & \text{If } T_2 \text{ is older than } T_1; \end{cases} \quad (1)$$

3.2. Circular statistics

Mardia and Jupp (2000) describe the Rayleigh test as a simple and powerful way to test for uniformity in circular distributions. The null hypothesis of a Rayleigh test is that the sample was derived from a circular-uniform distribution, versus the alternative that the distribution is not uniform. A circular-uniform distribution would imply no preferred orientation of the phase angle. As discussed by Mardia and Jupp (2000), it is

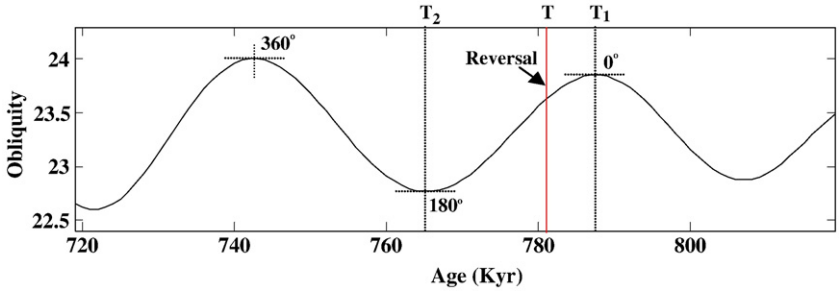

Fig. 2. Definition of phase of orbital cycles corresponding to a reversal/excursion.

Table 2
p-value of Rayleigh test for phase data in Figs. 3–5

Datasets	Actual obliquity	Actual eccentricity	Max. obliquity envelope
8 best-established excursions (Table 1)	0.231	0.922	0.080
Last 9 reversals in CK95 (Cande and Kent, 1995)	0.138	**0.036**	**0.039**
Last 9 reversals in ATNTS2004 (Lourens et al., 2004)	0.570	**0.009**	**0.023**
Reversals in CK95 (last 5 Myr) (Cande and Kent, 1995)	0.103	0.365	**0.036**
Reversals in ATNTS2004 (last 5 Myr) (Lourens et al., 2004)	0.157	0.847	**0.031**
Reversals in CK95 (12.5–8 Ma) (Cande and Kent, 1995)	0.751	0.741	0.095
Reversals in ATNTS2004 (12.5–8 Ma) (Lourens et al., 2004)	0.719	0.675	0.141
Husing et al. (2007) timescale (12.5–8 Ma)	0.105	0.744	0.142
Evans et al. (2007) timescale (12–9 Ma)	0.131	0.211	0.098
Reversals in CK95 (25–15 Ma) (Cande and Kent, 1995)	0.880	0.855	0.298
Reversals in ATNTS2004 (25–15 Ma) (Lourens et al., 2004)	0.857	0.943	0.954
Billups et al. (2004) timescale (25–15 Ma)	0.926	0.262	0.291
Pälike et al. (2006) timescale (25–15 Ma)	0.824	0.340	0.393
Reversals in CK95 (last 25 Myr) (Cande and Kent, 1995)	0.124	0.813	0.424
Reversals in ATNTS2004 (last 25 Myr) (Lourens et al., 2004)	0.317	0.519	0.980

In bold: *p*-values that are less than 0.05.

useful to take the Rayleigh test statistic as $2N\bar{R}^2$, where N is the number of phase data θ_i, and $\bar{R}$ is the mean resultant length defined as:

$$\bar{R} = \frac{1}{N}\sqrt{\left(\sum_{i=1}^{N}\cos\theta_i\right)^2 + \left(\sum_{i=1}^{N}\sin\theta_i\right)^2} \quad (2)$$

Mardia and Jupp (2000) report that the Rayleigh test statistic $2N\bar{R}^2$ is distributed as chi-squared with two degrees of freedom. The upper tail probabilities of $N\bar{R}^2$ (the *p*-value of Rayleigh test) can be approximated using the following equation:

$$\Pr\left(N\bar{R}^2 \geq K\right) = e^{-K}\left\{1 + \frac{2K - K^2}{4N} - \frac{24K - 132K^2 + 76K^3 - 9K^4}{288N^2}\right\} \quad (3)$$

By setting a significance level for the test (for instance, 0.05), we can decide to accept the uniform distribution hypothesis (*p*-value ≥ significance level) or reject it (*p*-value < significance level). The *p*-value of different datasets are calculated and listed in Table 2. For phase data that are not uniformly distributed, we can estimate the preferred phase angle or phase angle interval by assuming a Von Mises distribution. Jones (2006) developed a MATLAB program for the statistical analysis of circular data that includes Von Mises distribution fitting. Note that results from the Rayleigh tests (Table 2) are all based on the assumption that there is no age uncertainty in reversals/excursions or in orbital solutions.

3.3. Monte Carlo simulation

It is obvious that age uncertainty from both the reversal/excursion timescales and the astronomical solution will directly influence the phase value of the orbital cycle at the time of the reversal/excursion, and hence the *p*-value from the Rayleigh tests. As can be seen from Eq. (3), the size of the population of phase data used in the Rayleigh test will also influence the *p*-value. The following procedure is designed to estimate these influences.

1) Following Fuller (2006), we assume that phases are preferentially distributed between 0° and 180°, which is the decreasing part (maximum to minimum) of orbital cycles.
2) We generate N points (numbers of reversals/excursions used in Table 2, i.e. 8, 9, 22, 37, or 89) of phase data ($i = 1, 2, 3, \ldots, N$), which are evenly distributed between 0° and 180°, and calculate the Rayleigh test *p*-value p_0.
3) We choose an age uncertainty level u (e.g. ±5 kyr) and the orbital cycle c for testing (e.g. 41 kyr obliquity cycle).
4) For each phase point θ_i in 2), we add the age uncertainty:

$$\theta_i' = \theta_i + ((\mathrm{rand}(-u, u)/c) \times 360°) \quad (4)$$

Rand $(-u, u)$ means a uniform distributed random number between $-u$ and u.
5) We calculate the Rayleigh test *p*-value for the phase dataset $\theta_i'(i = 1, 2, 3, \ldots, N)$.
6) We repeat steps 4) and 5) 1,000,000 times, sort the calculated 1,000,000 *p*-values into an increasing series.
7) We find the maximum index of the sorted *p*-value series, corresponding to *p*-values that are less than $p_0 + 0.05$.
8) We calculate the percentage of *p*-values that are bigger than $p_0 + 0.05$ in the sorted *p*-value series: $[(1{,}000{,}000 - n)/1{,}000{,}000] \times 100\%$, where n is the maximum index number acquired from step 7).

This percentage value gives an estimate of the likelihood that such an age uncertainty would cause a change of the Rayleigh test *p*-value by >0.05. Percentage values for different age uncertainty levels, and for different numbers of data points in different orbital cycles, are calculated and listed in Table 3.

4. Results

In Fig. 3, we show the phases of actual orbital obliquity corresponding to ages for: (1) the eight best-established

Table 3
Monte Carlo simulation of influence of age uncertainties and number of data points on Rayleigh test *p*-value

	Data points	Original *p*-value	Age uncertainty level (kyr)						
			±5	±7.5	±10	±12.5	±15	±17.5	±20
Obliquity cycle (41 kyr)	8	0.088	46.7%	59.1%	68.5%	76.4%	81.9%	85.1%	86.2%
	9	0.056	43.1%	58.0%	69.2%	78.1%	84.5%	88.1%	89.4%
	10	0.036	38.5%	55.9%	68.9%	79.0%	86.0%	90.1%	91.4%
	22	0.000	0.2%	**9.3%**	34.3%	62.0%	81.8%	91.9%	94.9%
	37	0.000	0.0%	0.2%	**7.2%**	34.6%	69.0%	89.3%	94.9%
	114	0.000	0.0%	0.0%	0.0%	**0.4%**	19.4%	73.0%	94.6%
	Data points	Original *p*-value	Age uncertainty level (kyr)						
			±5	±10	±15	±20	±25	±30	±40
Eccentricity cycle (100 kyr)	8	0.088	19.2%	40.8%	52.9%	61.9%	69.4%	75.7%	84.0%
	9	0.056	11.9%	36.1%	50.7%	61.5%	70.2%	77.4%	86.9%
	10	0.036	**5.9%**	30.0%	47.2%	59.9%	70.1%	78.2%	88.6%
	22	0.000	0.0%	0.0%	**2.2%**	15.2%	37.3%	59.9%	88.5%
	37	0.000	0.0%	0.0%	0.0%	0.7%	**9.0%**	31.9%	82.6%
	114	0.000	0.0%	0.0%	0.0%	0.0%	0.0%	**0.3%**	49.7%
	Data points	Original *p*-value	Age uncertainty level (kyr)						
			±20	±50	±100	±200	±300	±400	±500
Max. obliquity envelope (~1.2 Myr)	8	0.088	**0.1%**	13.5%	35.2%	56.1%	69.5%	79.2%	84.7%
	9	0.056	0.0%	**7.0%**	29.5%	54.5%	70.2%	81.4%	87.7%
	10	0.036	0.0%	**2.5%**	22.6%	51.8%	70.1%	82.7%	89.6%
	22	0.000	0.0%	0.0%	0.0%	**5.1%**	37.1%	72.5%	90.8%
	37	0.000	0.0%	0.0%	0.0%	0.0%	**9.0%**	51.5%	87.1%
	114	0.000	0.0%	0.0%	0.0%	0.0%	0.0%	**3.9%**	65.0%

Original phase data are generated evenly between 0° and 180°. Using various populations of data points (corresponding to numbers of reversals/excursions in datasets of Table 2), 1,000,000 Monte Carlo simulations for each level of age uncertainty provided the percentage of simulations that have >0.05 difference in *p*-value from the original *p*-value. In bold: critical thresholds where small changes in the corresponded age uncertainty lead to large changes in *p*-value.

excursions in the Brunhes and Matuyama Chrons (Table 1); (2) the last 9 reversals (i.e. base of Brunhes, top and base of Jaramillo, top and base of Cobb Mountain, top and base of Olduvai, and top and base of Réunion) in CK95 (Cande and Kent, 1995) and ATNTS2004 (Lourens et al., 2004); (3) reversals of the last 5 Myr in CK95 and ATNTS2004; (4) reversals in the 12.5–8.5 Ma interval in CK95, ATNTS2004, Husing et al., (2007), and Evans et al., (2007); (5) reversals in the 25–15 Ma interval in CK95, ATNTS2004, Billups et al. (2004), and Pälike et al. (2006); and (6) reversals of the last 25 Myr in CK95 and ATNTS2004. Assuming no age uncertainty in reversal/excursion ages or in the astronomical solution, the *p*-values of the Rayleigh tests (Table 2) indicate that none of the data groups show any preferred phase distribution in the obliquity cycle at the 5% significance level, although reversal ages for the last 5 Myr have borderline significance (*p*-value=0.157 or 0.103 depending on timescale used, see Table 2). The Monte Carlo simulation indicates that a reversal age uncertainty of 5–15 kyr (depending on the number of reversal ages) causes large changes in the percentage values (Table 3), implying that reversal/excursion ages would have to be known within these tight constraints in order for a phase relationship to be resolvable. This conclusion is intuitively obvious in view of the brevity of the 41-kyr cycle relative to a reversal age uncertainty of 5–15 kyr. Uncertainties in reversal/excursion ages in current timescales exceed 5–15 kyr (with the exception of the two excursions known to have occurred in the last 50 kyrs) in part because the duration of the reversal transition itself probably exceeds 5 kyr. It is, therefore, very unlikely that a relationship between reversal age and orbital obliquity, were it to exist, would be resolvable.

A similar calculation has been carried out for orbital eccentricity (Fig. 4) assuming no age uncertainty in reversal/excursion ages or astronomical solution. The last 9 reversals seem to preferentially occur during the increasing part of eccentricity cycles (Fig. 4b and c) and the distribution of phases (*p*-value=0.009 or 0.036 depending on timescale used) is non-uniform at the 5% significance level (Table 2). This result is, however, not consistent with the Rayleigh test results from the compiled excursion ages or any other groupings of reversal ages (Table 2), for which no preferred phase angle is observed. The *p*-values of Rayleigh tests for phases of eccentricity and phases of the maximum obliquity envelope corresponding to different numbers of reversal ages (last 9 to last 36 reversals) are listed for CK95 and ATNTS2004 (Table 4). The preferred phase distribution in the eccentricity cycle at the 5% significance ceases when adding even one more reversal age beyond the last 9 reversals in CK95, or adding three more reversal ages in ATNTS2004 timescale. The Monte Carlo simulations for eccentricity cycles indicate that large changes in the percentage values (Table 3) occur when the age uncertainty is in the 10–40 kyr range, depending on the number of reversal/excursion ages in the simulation. For less than 10 reversal ages (the last 3 Myrs), age uncertainties of 10–20 kyr are sufficient to inhibit the recognition of a relationship between reversal/excursion age and phase of eccentricity. This is deduced from the change in the percentage

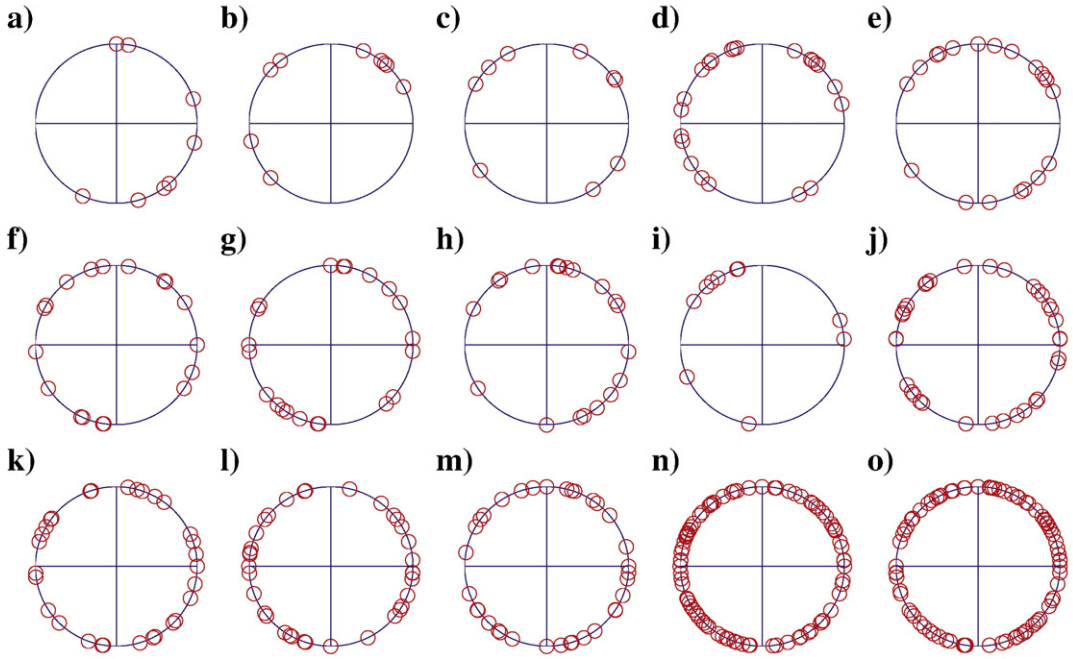

Fig. 3. Circular plot of phase of *actual obliquity* (Laskar et al., 2004) for: a) 8 best-established excursions (Table 1); b) Last 9 reversals in CK95 (Cande and Kent, 1995); c) Last 9 reversals in ATNTS2004 (Lourens et al., 2004); d) Reversals in CK95 (last 5 Myr) (Cande and Kent, 1995); e) Reversals in ATNTS2004 (last 5 Myr) (Lourens et al., 2004); f) Reversals in CK95 (12.5–8 Ma) (Cande and Kent, 1995); g) Reversals in ATNTS2004 (12.5–8 Ma) (Lourens et al., 2004); h) Husing et al. (2007) timescale (12.5–8 Ma); i) Evans et al. (2007) timescale (12–9 Ma); j) Reversals in CK95 (25–15 Ma) (Cande and Kent, 1995); k) Reversals in ATNTS2004 (25–15 Ma) (Lourens et al., 2004); l) Billups et al. (2004) timescale (25–15 Ma); m) Pälike et al. (2006) timescale (25–15 Ma); n) Reversals in CK95 (last 25 Myr) (Cande and Kent, 1995); o) Reversals in ATNTS2004 (last 25 Myr) (Lourens et al., 2004). Phase angles of 0° (or 360°), 90°, 180°, 270° are marked by lines clockwise from top of each circular plot.

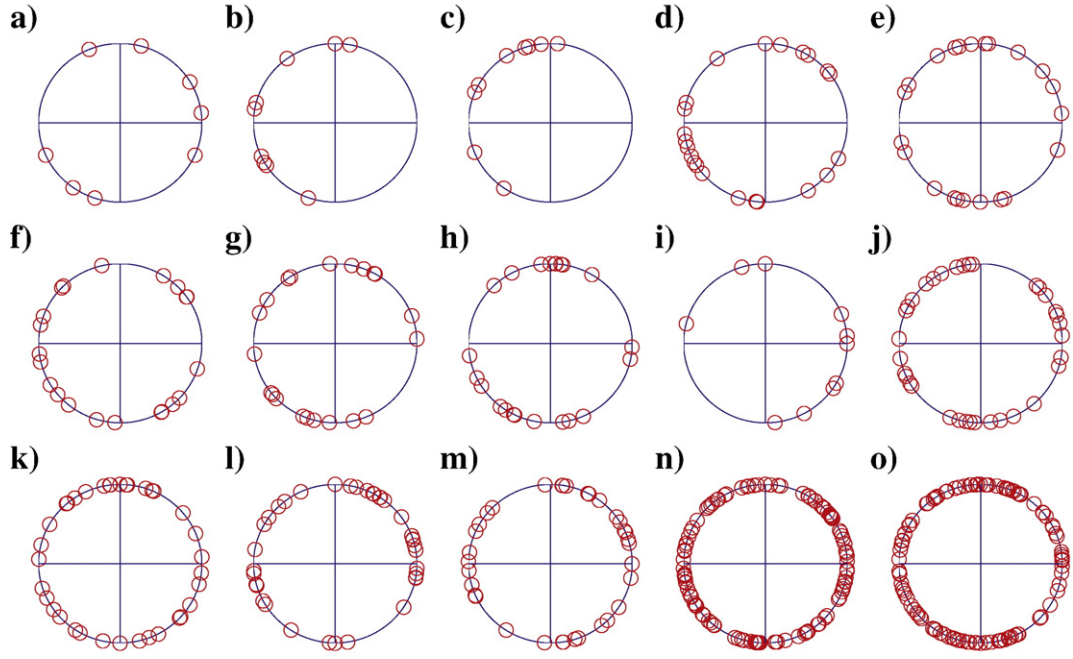

Fig. 4. Circular plot of phase of *actual eccentricity* (Laskar et al., 2004) for: a) 8 best-established excursions (Table 1); b) Last 9 reversals in CK95 (Cande and Kent, 1995); c) Last 9 reversals in ATNTS2004 (Lourens et al., 2004); d) Reversals in CK95 (last 5 Myr) (Cande and Kent, 1995); e) Reversals in ATNTS2004 (last 5 Myr) (Lourens et al., 2004); f) Reversals in CK95 (12.5–8 Ma) (Cande and Kent, 1995); g) Reversals in ATNTS2004 (12.5–8 Ma) (Lourens et al., 2004); h) Husing et al. (2007) timescale (12.5–8 Ma); i) Evans et al. (2007) timescale (12–9 Ma); j) Reversals in CK95 (25–15 Ma) (Cande and Kent, 1995); k) Reversals in ATNTS2004 (25–15 Ma) (Lourens et al., 2004); l) Billups et al. (2004) timescale (25–15 Ma); m) Pälike et al. (2006) timescale (25–15 Ma); n) Reversals in CK95 (last 25 Myr) (Cande and Kent, 1995); o) Reversals in ATNTS2004 (last 25 Myr) (Lourens et al., 2004). Phase angles of 0° (or 360°), 90°, 180°, 270° are marked by lines clockwise from top of each circular plot.

Table 4
p-value of Rayleigh tests for phases of eccentricity and maximum obliquity envelope corresponding to different number of reversal ages (last 9 to last 36 reversals) in CK95 (Cande and Kent, 1995) and ATNTS2004 time scale (Lourens et al., 2004)

Reversal numbers	Eccentricity		Obliquity envelope	
	CK95	ATNTS04	CK95	ATNTS04
9 (2148)	0.036	0.009	0.039	0.023
10 (2581)	0.105	0.016	0.121	0.088
11 (3032)	0.146	0.027	0.205	0.155
12 (3116)	0.218	0.104	0.217	0.159
13 (3207)	0.376	0.202	0.138	0.101
14 (3330)	0.448	0.158	0.070	0.049
15 (3596)	0.359	0.309	0.083	0.067
16 (4187)	0.548	0.478	0.075	0.058
17 (4300)	0.743	0.531	0.044	0.032
18 (4493)	0.885	0.363	0.022	0.016
19 (4631)	0.734	0.553	0.013	0.010
20 (4799)	0.563	0.553	0.015	0.011
21 (4896)	0.517	0.746	0.021	0.016
22 (4997)	0.365	0.847	0.036	0.031
23 (5235)	0.504	0.930	0.086	0.077
24 (6033)	0.689	0.833	0.055	0.080
25 (6252)	0.544	0.912	0.083	0.155
26 (6436)	0.634	0.805	0.159	0.236
27 (6733)	0.799	0.782	0.169	0.164
28 (7140)	0.902	0.911	0.109	0.165
29 (7212)	0.811	0.802	0.089	0.185
30 (7251)	0.870	0.911	0.077	0.206
31 (7285)	0.911	0.800	0.069	0.226
32 (7454)	0.978	0.704	0.088	0.304
33 (7489)	0.912	0.580	0.111	0.392
34 (7528)	0.942	0.690	0.146	0.489
35 (7642)	0.846	0.571	0.216	0.620
36 (7695)	0.761	0.587	0.319	0.751

Inside the parentheses are reversal ages (in kyr) from ATNTS2004 timescale corresponding to the reversal number to the left of the parentheses.

values as reversal/excursion age uncertainty increases (Table 3). As a test, we replace the Réunion ages (both top and base) in CK95 and ATNTS2004, derived from the cylostratigraphies in the Italian sections (Zijderveld et al., 1991; Lourens et al., 1996), with more recent Réunion ages from ODP Site 981 (Channell et al., 2003). The results indicate that *p*-values for eccentricity phases corresponding to the last 9 reversals change from 0.036 to 0.147 for CK95, and from 0.009 to 0.033 using ATNTS2004. This indicates the sensitivity of the Rayleigh tests to estimates of the age of (Réunion) reversals that differ by 5–25 kyr. According to the simulations, when larger populations of reversal ages back to 25 Ma are considered, age uncertainties up to 40 kyr are sufficient to inhibit the recognition of any phase relationship that may be present. It is unlikely that reversal ages older than 5 Ma in current timescales are known with uncertainties less than 40 kyr. For example, differences between polarity chron ages in ATNTS2004 (Lourens et al., 2004) and the later Billups et al. (2004) timescale exceed 200 kyr in the Early Miocene (Fig. 1). Any relationship between reversal age and the phase of orbital eccentricity is unlikely to be resolvable, at least beyond the last 5 Myrs. For the last nine reversals, the Rayleigh test (p-value = 0.009 or 0.036, Table 2) indicates a preferred phase distribution in the eccentricity cycle at the 5% significance level, however, in view of the simulations, this implies that reversal ages for the last 3 Myr are known to within ~15 kyr.

To analyze the relationship between reversal/excursion age and ~1.2 Myr modulation envelope of the orbital obliquity, the envelope data were smoothed using the Savitzky–Golay smoothing filter (Savitzky and Golay, 1964), a time-domain smoothing based on a least squares polynomial fit across a moving window applied to the dataset. From Table 2 and Fig. 5, considering no age uncertainty in reversal/excursion ages or orbital solution, we see that the phases corresponding to the last 9 reversals (Fig. 5b and c) and reversals in the last 5 Myr (Fig. 5d and e) are not uniformly distributed (i.e. have preferential phase) at the 5% significance level (Table 2). A preferred relationship with the maximum obliquity envelope is also indicated for the eight best-established excursion ages (Table 1) by the relatively low p-value (0.080) from the Rayleigh test (Table 2), although it is not significant at the 5% level. Note that even a manually generated 8-point phase dataset that is evenly distributed between 0° and 180° has a Rayleigh test p-value of 0.088 (Table 3). The compiled excursion ages (Table 1) might not be appropriate for exploring a phase distribution in the maximum obliquity envelope because: 1) these excursion ages only span the 1.115–0.033 Ma interval, with a duration that is even shorter than a maximum obliquity envelope cycle; 2) these excursions were chosen based on their age quality, with no excursions included in the 0.850–0.211 Ma interval. In this case, in the Monte Carlo simulations, the percentage of simulations that have $p > 0.05$ at the 50 kyr age uncertainty level (Table 3) is small (~13.5% for 8 data points, ~7.0% for 9 data points, and ~0% for 22 data points). According to the simulations, the result is not influenced by age uncertainties unless these age uncertainties exceed 50 kyr (for the 8 excursions or the last 9 reversals, Table 3) or 200 kyr for last 5 Myrs (Table 3). Assuming a Von Mises distribution for phases corresponding to reversals during the last 5 Myrs (in ATNTS2004 timescale), a mean phase of 103.5°, and a 95% confidence interval between 56.0° and 151.1° is obtained using the MATLAB protocol (Jones, 2006). In contrast to Fuller's conclusion (Fuller, 2006) that reversals preferentially occurred when the average amplitude of the obliquity signal is lower than the mean, this result implies that, in the last 5 Myrs, reversals preferentially occurred during decrease of the maximum obliquity envelope. The results of the Rayleigh test do not hold, however, when we consider reversal ages back to 25 Ma or other groupings of reversal ages (Fig. 5f–o). Results from Table 4 indicate that the preferential distribution of reversal ages with phase of the maximum obliquity envelope for the last 5 Myr breaks down when adding even one more reversal age using either CK95 or ATNTS2004. The inconsistency could be attributed to larger than expected reversal age uncertainties beyond 5 Ma combined with a link between reversal age and phase of the obliquity envelope cycle. Note that the maximum difference between reversal ages for the 25–15 Ma interval in the ATNTS2004 (Lourens et al., 2004) and Billups et al. (2004) timescales reaches 230 kyr (Fig. 1).

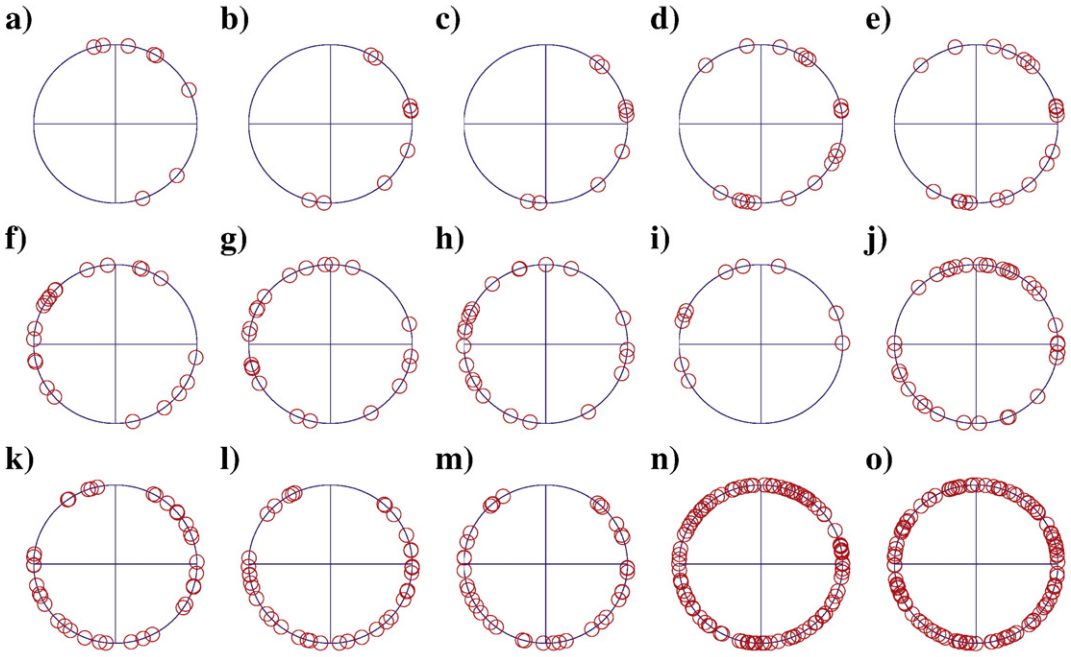

Fig. 5. Circular plot of phase of *maximum obliquity envelope* for: a) 8 best-established excursions (Table 1); b) Last 9 reversals in CK95 (Cande and Kent, 1995); c) Last 9 reversals in ATNTS2004 (Lourens et al., 2004); d) Reversals in CK95 (last 5 Myr) (Cande and Kent, 1995); e) Reversals in ATNTS2004 (last 5 Myr) (Lourens et al., 2004); f) Reversals in CK95 (12.5–8 Ma) (Cande and Kent, 1995); g) Reversals in ATNTS2004 (12.5–8 Ma) (Lourens et al., 2004); h) Husing et al. (2007) timescale (12.5–8 Ma); i) Evans et al. (2007) timescale (12–9 Ma); j) Reversals in CK95 (25–15 Ma) (Cande and Kent, 1995); k) Reversals in ATNTS2004 (25–15 Ma) (Lourens et al., 2004); l) Billups et al. (2004) timescale (25–15 Ma); m) Pälike et al. (2006) timescale (25–15 Ma); n) Reversals in CK95 (last 25 Myr) (Cande and Kent, 1995); o) Reversals in ATNTS2004 (last 25 Myr) (Lourens et al., 2004). Phase angles of 0° (or 360°), 90°, 180°, 270° are marked by lines clockwise from top of each circular plot.

The Monte Carlo simulations (Table 3) indicate that, for the larger populations of reversal ages in the 25–15 Ma interval (37 reversals), >300 kyr age uncertainties would drive the simulated *p*-value to values indicative of a uniform distribution of phases.

5. Conclusions

Fuller (2006) made several observations linking the paleomagnetic records to orbital solutions for obliquity: (1) Several paleointensity minima in the Sint-800 paleointensity

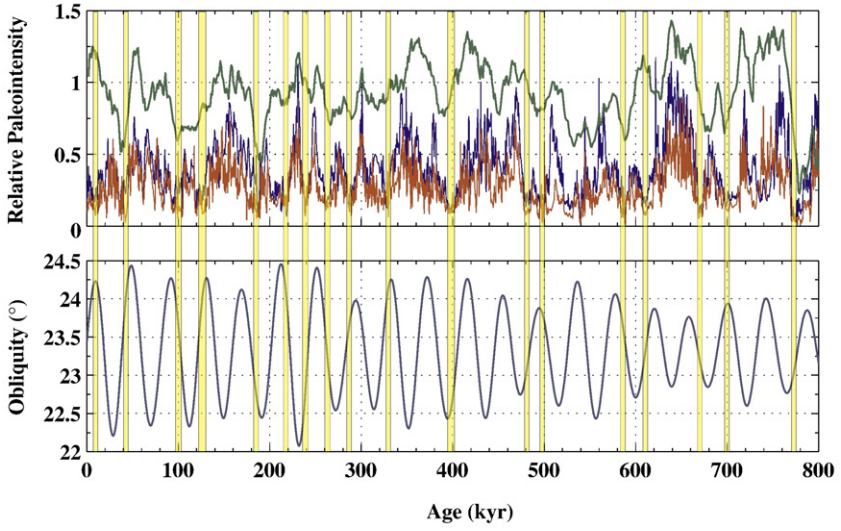

Fig. 6. Comparing relative paleointensity records with orbital obliquity during the last 800 kyr. Top panel: Sint-800 record (Guyodo and Valet, 1999) in green, ODP 983 paleointensity record (Channell, 1999; Channell and Kleiven, 2000;Channell et al., 1997) in blue, and ODP 984 paleointensity record (Channell, 1999; Channell et al., 2004) in red. Bottom panel: orbital obliquity signal from Laskar et al. (2004). (For interpretation of the references to color in this figure legend, the reader is referred to the web version of this article.)

stack (Guyodo and Valet, 1999) correlate with individual obliquity minima, (2) The durations of polarity chrons in the ATNTS2004 timescale (Lourens et al., 2004) display a peak at 30–40 kyr. (3) The last 9 reversals occurred at a preferred phase in the obliquity cycle. (4) The last 17 reversals occurred preferentially during minima in the orbital obliquity envelope.

A relationship between paleointensity lows in the Sint-800 stack and the obliquity minima is difficult to establish due to uncertainties in the chronology of the stack that must approach the obliquity period (Guyodo and Valet, 1999; McMillan et al., 2004). Correlations of the obliquity signal with prominent lows in individual paleointensity records from ODP Site 983 (Channell, 1999; Channell and Kleiven, 2000; Channell et al., 1997) and Site 984 (Channell, 1999; Channell et al., 2004), that have oxygen isotope age control, do not show any obvious pattern (Fig. 6).

The distribution of polarity chron durations in the ATNTS2004 timescale (point 2, above) can be attributed to the Poisson distribution of polarity chron durations, combined with truncation of low duration values in the timescale as a result of the resolution of the MMA data on which the template for polarity reversal is largely based. The pattern of polarity chrons in ATNTS2004 is essentially inherited from MMA data where the practical lower limit of duration for polarity chron recognition is ~30 kyr (Cande and Kent, 1995).

The Rayleigh test is used to determine the likelihood of a relationship of reversal/excursion ages to the phases of obliquity, eccentricity and obliquity envelope. Assuming no age uncertainty in reversal/excursion ages or astronomical solution, small *p*-values in the Rayleigh test indicate a non-uniform distribution of phases (bold in Table 2). Although there is a significant relationship (at 5% level) between the last 9 reversals and phase of eccentricity cycles, the relationship breaks down when adding 1 or 3 additional reversal ages, depending on polarity timescale used (Table 4). The relationship was not observed for any other groupings of reversal ages, or for a compilation of excursion ages (Fig. 4). Monte Carlo simulations demonstrate that these tests are very sensitive to reversal age uncertainties and may be biased by reversal age uncertainties as low as 5 kyr in the case of obliquity at low reversal populations, to 40 kyr for eccentricity at higher reversal populations extending back to 25 Ma. A conservative estimate for reversal age uncertainties beyond 5 Ma is 40 kyr (one obliquity cycle) and for the last 5 Myr the reversal age uncertainties certainly exceed 10 kyr. For this reason, we consider that any relationship between reversal age and the phase of obliquity or eccentricity would not be resolvable due to imprecision in reversal ages.

Considering no age uncertainty in reversal/excursion ages or astronomical solution, the phase of the maximum obliquity envelope at times of the last 9 reversals, and reversals in last 5 Myr, are not uniformly distributed at the 5% significance level. Polarity reversals younger than 5 Ma preferentially occur during decrease in amplitude of the envelope, rather than when the obliquity is lower than the mean (as deduced by Fuller (2006)). This significant relationship for the last 5 Myr does not hold when adding even one additional reversal age to the test (Table 4), or when applied to other groupings of reversal ages (Fig. 5). The Monte Carlo simulations indicate that uncertainties in reversal/excursion age and/or orbital solution for the small reversal population back to 5 Ma would have to exceed 50–100 kyr to account for the test result in the presence of a phase relationship similar to that advocated by Fuller (2006). The reversal age uncertainties would have to lie in the 300–500 kyr range to account for the test results for reversal populations extending back to 25 Ma (Table 3). We would not expect reversal ages to be sufficiently imprecise to influence this result for the last 5 Myr, however, the difference between the ATNTS2004 (Lourens et al., 2004) and Billups et al. (2004) reversal ages reach 230 kyr in the Early Miocene (Fig. 1), indicating that reversal age uncertainties may reach several hundred kyrs for reversals older than 5 Myr. Inconsistency of the relationship between phase of obliquity envelope and reversal age for the last 5 Myr, and for other time intervals, could be attributed to larger than expected reversal age uncertainties beyond 5 Ma *and* a link between reversal age the obliquity envelope, or, more probably, the fortuitous occurrence of a low probability relationship over the last 5 Ma that has no mechanistic implication.

Acknowledgement

The authors thank the journal reviewers and Mark Yang for comments that improved the manuscript. Research supported by NSF OCE 0350830.

References

Benson, L., Liddicoat, J., Smoot, J., Sarna-Wojcicki, A., Negrini, R., Lund, S., 2003. Age of the Mono Lake excursion and associated tephra. Quat. Sci. Rev. 22, 135–140.

Billups, K., Pälike, H., Channell, J.E.T., Zachos, J.C., Shackleton, N.J., 2004. Astronomic calibration of the late Oligocene through early Miocene geomagnetic polarity time scale. Earth Planet. Sci. Lett. 224, 33–44.

Blackett, P.M.S., 1952. A negative experiment relating magnetism and the Earth's rotation. Philos. Trans. R. Soc. Lond. Ser. A 245, 309–370.

Cande, S.C., Kent, D.V., 1992. A new geomagnetic polarity time scale for the late Cretaceous and Cenozoic. J. Geophys. Res. 97, 13917–13951.

Cande, S.C., Kent, D.V., 1995. Revised calibration of the geomagnetic polarity time scale for the Late Cretaceous and Cenozoic. J. Geophys. Res. 100, 6093–6095.

Channell, J.E.T., 1999. Geomagnetic paleointensity and directional secular variation at Ocean Drilling Program (ODP) Site 984 (Bjorn Drift) since 500 ka: comparisons with ODP Site 983 (Gardar Drift). J. Geophys. Res. 104, 22937–22951.

Channell, J.E.T., Kleiven, H.F., 2000. Geomagnetic paleointensities and astrochronological ages for the Matuyama-Brunhes boundary and the boundaries of the Jaramillo Subchron: palaeomagnetic and oxygen isotope records from ODP Site 983. Phil. Trans. R. Soc. Lond. A 358, 1027–1047.

Channell, J.E.T., Hodell, D.A., Lehman, B., 1997. Relative geomagnetic paleointensity and $\delta^{18}O$ at ODP Site 983 (Gardar Drift, North Atlantic) since 350 ka. Earth Planet. Sci. Lett. 153, 103–118.

Channell, J.E.T., Hodell, D.A., McManus, J., Lehman, B., 1998. Orbital modulation of the Earth's magnetic field intensity. Nature 394, 464–468.

Channell, J.E.T., Mazaud, A., Sullivan, P., Turner, S., Raymo, M.E., 2002. Geomagnetic excursions and paleointensities in the Matuyama Chron at ODP Sites 983 and 984 (Iceland Basin). J. Geophys. Res. 107. doi:10.1029/2001JB000491.

Channell, J.E.T., Labs, J., Raymo, M.E., 2003. The Réunion Subchronozone at ODP Site 981 (Feni Drift, North Atlantic). Earth Planet. Sci. Lett. 215, 1–12.

Channell, J.E.T., Curtis, J.H., Flower, B.P., 2004. The Matuyama-Brunhes boundary interval (500–900 ka) in North Atlantic drift sediments. Geophys. J. Int. 158, 489–505.

Evans, H.F., Westerhold, T., Paulsen, H., Channell, J.E.T., 2007. Astronomical ages for Miocene polarity chrons C4Ar–C5r (9.3–11.2 Ma), and for three excursion chrons within C5n.2n. Earth Planet. Sci. Lett. 256, 455–465.

Fuller, M., 2006. Geomagnetic field intensity, excursions, reversals and the 41,000-yr obliquity signal. Earth Planet. Sci. Lett. 245, 605–615.

Guyodo, Y., Valet, J.P., 1999. Global changes in intensity of the Earth's magnetic field during the past 800 kyr. Nature 399, 249–252.

Guyodo, Y., Gaillot, P., Channell, J.E.T., 2000. Wavelet analysis of relative geomagnetic paleointensity at ODP Site 983. Earth Planet. Sci. Lett. 184, 109–123.

Hilgen, F.J., 1991. Extension of the astronomically calibrated (polarity) time scale to the Miocene/Pliocene boundary. Earth Planet. Sci. Lett. 107, 349–368.

Husing, S.K., Hilgen, F.J., Abdul Aziz, H., Krijgsman, W., 2007. Completing the Neogene geological time scale between 8.5 and 12.5 Ma. Earth Planet. Sci. Lett. 253, 340–358.

Jones, T.A., 2006. MATLAB functions to analyze directional (azimuthal) data-I: single-sample inference. Comput. Geosci. 32, 166–175.

Kent, D.V., 1982. The apparent correlation of paleomagnetic intensity and climate records in deep sea sediments. Nature 299, 538–540.

Kent, D.V., Carlut, J., 2001. A negative test of orbital of geomagnetic reversals and excursions. Geophys. Res. Lett. 28, 3561–3564.

Kent, D.V., Opdyke, N.D., 1977. Paleomagnetic field intensity variation recorded in a Brunhes epoch deep sea sediment core. Nature 266, 156–159.

Laj, C., Kissel, C., Mazaud, A., Channell, J.E.T., Beer, J., 2000. North Atlantic paleointensity stack since 75 ka (NAPIS-75) and the duration of the Laschamp event. Phil. Trans. R. Soc. Lond. A 358, 1009–1025.

Langereis, C.G., Dekkers, M.J., de Lange, G.J., Paterne, M., van Santvoort, P.J.M., 1997. Magnetostratigraphy and astronomical calibration of the last 1.1 Myr from an eastern Mediterranean piston core and dating of short events in the Brunhes. Geophys. J. Int. 129, 75–94.

Laskar, J., 1990. The chaotic motion of the Solar System: a numerical estimate of the size of the chaotic zones. Icarus 88, 266–291.

Laskar, J., Joutel, F., Boudin, F., 1993. Orbital, precessional, and insolation quantities for the Earth from 220 Myr to 110 Myr. Astron. Astrophys. 270, 522–533.

Laskar, J., Robutel, P., Joutel, F., Gastineau, M., Correia, A., Levrard, B., 2004. A long term numerical solution for the insolation quantities of the Earth. Astron. Astrophys. 428, 261–285.

Loper, D.E., 1975. Torque balance and energy budget for the precessionally driven dynamo. Phys. Earth Planet. Inter. 11, 43–60.

Lourens, L., Hilgen, F., Laskar, J., Shackleton, N., Wilson, D., 2004. The Neogene period. In: Gradstein, F., Ogg, J., et al. (Eds.), A Geologic Time Scale. Cambridge University Press, pp. 409–440.

Lourens, L.J., Antonarakou, A., Hilgen, F.J., Van Hoof, A.A.M., Vergnaud-Grazzini, C., Zachariasse, W.J., 1996. Evaluation of the Plio-Pleistocene astronomical timescale. Paleoceanography 11, 391–413.

Malkus, W.V.R., 1968. Precession of the Earth as a cause of geomagnetism. Science 169, 259–264.

Mardia, K.V., Jupp, P.E., 2000. Directional Statistics. Wiley, Chichester, UK. 429pp.

McMillan, D., Constable, C., Parker, R., 2004. Assessing the dipolar signal in stacked paleointensity records using a statistical error model and geodynamo simulations. Phys. Earth Planet. Inter. 145, 37–54.

Pälike, H., Laskar, J., Shackleton, N.J., 2004. Geologic constraints on the chaotic diffusion of the Solar System. Geology 32, 929–932.

Pälike, H., Norris, R.D., Herrle, J.O., Wilson, P.A., Coxall, H.K., Lear, C.H., Shackleton, N.J., Tripati, A.K., Wade, B.S., 2006. The heartbeat of the Oligocene climate system. Science 314, 1894–1898.

Roberts, A.P., Winklhofer, M., Liang, W., Horng, C., 2003. Testing the hypothesis of orbital (eccentricity) influence on Earth's magnetic field. Earth Planet. Sci. Lett. 216, 187–192.

Rochester, M.G., Jacobs, J.A., Smylie, D.E., Chong, K.F., 1975. Can precession power the geomagnetic dynamo? Geophys. J. R. Astron. Soc. 43, 661–678.

Savitzky, A., Golay, M.J.E., 1964. Smoothing and differentiation of data by simplified least squares procedures. Anal. Chem. 36, 1627–1639.

Shackleton, N.J., Berger, A., Peltier, W.R., 1990. An alternative astronomical calibration of the lower Pleistocene timescale based on ODP Site 677. Trans. R. Soc. Edin. Earth Sci. 81, 251–261.

Shackleton, N.J., Crowhurst, S., Hagelberg, T., Pisias, N.G., Schneider, D.A., 1995. A new Late Neogene time scale: application to Leg 138 sites. In: Pisias, N.G., Mayer, L.A., Janecek, T.R., Palmer-Julson, A., van Andel, T.H. (Eds.), Proc. ODP, Sci. Results, vol. 138. Ocean Drilling Program, College Station, TX, pp. 73–101.

Singer, B.S., Brown, L.L., Rabassa, J.O., Guillou, H., 2004. $^{40}Ar/^{39}Ar$ chronology of late Pliocene and Early Pleistocene geomagnetic and glacial events in southern Argentina. In: Channell, J.E.T., et al. (Eds.), Timescales of the Paleomagnetic Field. AGU Geophysical Monograph Series, vol. 145, pp. 175–190.

Singer, B.S., Jicha, B.R., Kirby, B.T., Geissman, J.W., Herrero-Bervera, E., in press. $^{40}Ar/^{39}Ar$ dating links Albuquerque Volcanoes to the Pringle Falls excursion and the geomagnetic instability time scale. Earth Planet. Sci. Lett.

Tilgner, A., 2005. Precession driven dynamos. Phys. Fluids 17, 034104.

Tric, E., Laj, C., Valet, J., Tucholke, P., Paterne, P., Guichard, F., 1991. The Blake geomagnetic event: transition geometry, dynamical characteristics and geomagnetic significance. Earth Planet. Sci. Lett. 102, 1–13.

Vanyo, J.P., Dunn, J.R., 2001. Core precession flow structure and energy. Geophys. J. Int. 142, 409–425.

Yamazaki, T., 1999. Relative paleointensity of the geomagnetic field during Brunhes Chron recorded in North Pacific deep-sea sediment cores: orbital influence? Earth Planet. Sci. Lett. 169, 23–35.

Yamazaki, T., Oda, H., 2002. Orbital influence on Earth's magnetic field: 100,000-year periodicity in inclination. Science 295, 2435–2438.

Zijderveld, J.D.A., Hilgen, F.J., Langereis, C.G., Verhallen, P.J.J.M., Zachariasse, W.J., 1991. Integrated magnetostratigraphy and biostratigraphy of the upper Pliocene–lower Pleistocene from the Monte Singa and Crotone areas in Calabria, Italy. Earth Planet. Sci. Lett. 107, 697–714.